51st IEEE Conference on Decision and Control
December 10-13, 2012. Maui, Hawaii, USA

GES Integrated LBL/USBL Navigation System for Underwater Vehicles

Pedro Batista, Carlos Silvestre, and Paulo Oliveira

Abstract— **This paper presents a novel navigation system based on the integration of a combined Long Baseline / Ultra Short Baseline (LBL/USBL) acoustic positioning system. First, an Attitude and Heading Reference System is proposed that relies solely on the LBL/USBL and a triad of rate gyros, avoiding the use of magnetometers, with globally exponentially stable (GES) error dynamics. A position and ocean current estimation solution is then introduced, which is fed by the position fixes obtained from the LBL/USBL and relative linear velocity measurements, provided by a Doppler velocity log (DVL). The resulting overall navigation system consists in a cascade system with GES error dynamics. Finally, simulation results are presented and discussed in order to evaluate the performance of the proposed solution.**

I. Introduction

While the use of the Global Positioning System (GPS) is widespread in the design of navigation solutions for aerial or ground vehicles, underwater vehicles require alternative sensors due to the strong attenuation that the electromagnetic field suffers in water. Solutions based on Long Baseline (LBL) and Short Baseline (SBL) acoustic positioning systems have been long pursued, see e.g. [1], [2], [3], [4], [5], and references therein. Position and linear velocity globally asymptotically stable (GAS) filters based on an Ultra-Short Baseline (USBL) positioning system were presented by the authors in [6], while the Extended Kalman Filter (EKF) is the workhorse of the solution presented in [7].

With a Long Baseline acoustic positioning system, an underwater vehicle has access to the distances to a set of known transponders, which are usually fixed in the mission scenario. With some mild assumptions on the LBL configuration, it is possible to determine the inertial position of the vehicle. With an Ultra-Short Baseline acoustic position system installed on-board the vehicle, in the so-called inverted configuration, see [8], the vehicle has access to the distance to a fixed transponder in the mission scenario and the time (or range) differences of arrival between each pair of receivers of the USBL array. From those measurements, and under some mild assumptions on the USBL array configuration, the position of the external landmark relative to the vehicle, and expressed in body-fixed coordinates, is readily available.

This work was partially supported by the FCT [PEst-OE/EEI/LA0009/2011] and by the EU Project TRIDENT (Contract No. 248497).

The authors are with the Institute for Systems and Robotics, Instituto Superior Técnico, Universidade Técnica de Lisboa, Av. Rovisco Pais, 1049-001 Lisboa, Portugal. Carlos Silvestre is also with the Department of Electrical and Computer Engineering, Faculty of Science and Technology of the University of Macau.
{pbatista,cjs,pjcro}@isr.ist.utl.pt

Using spread spectrum techniques, see [9], it is possible to combine LBL and USBL acoustic positioning devices, which gives, in essence, both the distance between the vehicle and each of the external landmarks and the time (or range) differences of arrival between pairs of receivers, for each landmark. The goal of this paper is to design a novel navigation filter based on all this information, in addition to relative velocity readings provided by a Doppler Velocity Log (DVL) and angular velocity measurements, possibly corrupted by bias, as provided by a triad of rate gyros. The contribution is twofold: i) a novel Attitude and Heading Reference System (AHRS) is proposed based on the LBL/USBL acoustic positioning system, with globally exponentially stable error (GES) dynamics; and ii) a filter for estimation of linear motion quantities is presented, also based on the LBL/USBL acoustic positioning system, and the overall cascade navigation system is shown to be GES.

The topic of attitude estimation is still very active, as evidenced by the large number of recent publications, see e.g. [10], [11], [12], [13]. The Extended Kalman Filter (EKF) has been at the core of numerous stochastic solution, see e.g. [14], while nonlinear alternatives, aiming for stability and convergence properties, have been proposed in [15], [16], [17], [18], [19], and [20], to mention just a few, see [21] for a thorough survey on attitude estimation. Recently, the authors have proposed two alternative solutions in [22] and [23]. In the first, the Kalman filter is the workhorse but no linearizations are carried out whatsoever, resulting in a design with guarantee of globally asymptotically stable (GAS) error dynamics. In the later, a cascade observer is proposed that achieves GES error dynamics and that requires less computational power than the Kalman filter, at the expense of filtering performance. Common to both solutions is the fact that the topological restrictions of the Special Orthogonal Group $SO(3)$ are not explicitly imposed, though they are verified asymptotically in the absence of noise. In the presence of sensor noise, the distance of the estimates provided by the cascade observer or the Kalman filter to $SO(3)$ remains close to zero and methods are proposed that give estimates of the attitude arbitrarily close to $SO(3)$. In [24] an alternative additional result gives attitude estimates explicitly on $SO(3)$, at the possible expense of continuity of the solution during the initial transients, hence not violating the topological limitations that are thoroughly discussed in [25].

The LBL/USBL acoustic system gives, in addition to the inertial position of the vehicle, measurements of body-fixed vectors corresponding to constant known inertial vectors, hence providing the necessary information for attitude estimation. With the addition of angular velocity measurements, possibly corrupted by bias, it is thus possible to devise a filtering solution for both the attitude and the rate gyro bias. This is, to the best of the authors' knowledge, the first attitude estimation solution based on a combined LBL/USBL system. In comparison with common solutions that resort to gravity and magnetic field measurements, the proposed alternative has the advantage of not requiring the measurement of the magnetic field, which may be disturbed in intervention scenarios near objects with strong magnetic signatures, rendering it useless for attitude estimation. Using the information of the attitude it is also possible to additionally incorporate the USBL measurements in the determination of the inertial position of a vehicle in the LBL system, hence the overall filter results in a cascade system. The stability is trivially established resorting to input-to-state stability concepts.

The paper is organized as follows. The attitude estimation problem that is considered in this paper is introduced in Section II, while the design of the Attitude and Heading Reference System is detailed in Section III. The overall navigation system, including linear and angular motion estimation, is presented in Section IV and its stability is briefly discussed. Simulation results are presented in Section V and Section VI summarizes the main conclusions of the paper.

A. Notation

The symbol $\mathbf{0}$ denotes a matrix (or vector) of zeros, $\mathbf{I}$ the identity matrix, and $\mathbf{blkdiag}(\mathbf{A}_1, \ldots, \mathbf{A}_n)$ a block diagonal matrix, all assumed of appropriate dimensions. The rank of matrix $\mathbf{X}$ is denoted by $\operatorname{rank}(\mathbf{X})$. For $\mathbf{x}, \mathbf{y} \in \mathbb{R}^3$, the cross product is represented by $\mathbf{x} \times \mathbf{y}$.

II. Problem Statement

Consider an underwater vehicle moving in a scenario where there is a set of fixed landmarks installed in a Long Baseline configuration and suppose that the vehicle is equipped with an Ultra Short Baseline acoustic positioning system, as depicted in Fig. 1. For further details on the USBL, the reader is referred to [8], [9], and references therein. Further assume that the vehicle has a set of three orthogonally mounted rate gyros installed on-board and a DVL. Finally, suppose that the vehicle is moving in the presence of unknown constant ocean currents. The problem considered in the paper is the design of a navigation filter, yielding position, attitude, ocean current velocity, and rate gyro bias estimates, with globally asymptotically stable error dynamics.

A. System dynamics

In order to set the problem framework, let $\{I\}$ denote an inertial reference coordinate frame and $\{B\}$ a coordinate frame attached to the vehicle, commonly denominated as the body-fixed reference frame. The linear motion of the vehicle is given by $\dot{\mathbf{p}}(t) = \mathbf{R}(t)\mathbf{v}(t)$, where $\mathbf{p}(t) \in \mathbb{R}^3$ denotes the inertial position of the vehicle, $\mathbf{v}(t) \in \mathbb{R}^3$ is the velocity of the vehicle relative to $\{I\}$ and expressed in body-fixed

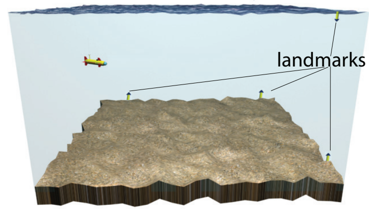

(a) AUV and LBL array

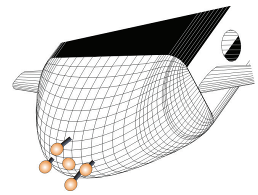

(b) AUV with USBL array

Fig. 1. Mission Scenario

coordinates, and $\mathbf{R}(t) \in SO(3)$ is the rotation matrix from $\{B\}$ to $\{I\}$, which satisfies $\dot{\mathbf{R}}(t) = \mathbf{R}(t)\mathbf{S}(\boldsymbol{\omega}(t))$, where $\boldsymbol{\omega}(t) \in \mathbb{R}^3$ is the angular velocity of $\{B\}$, expressed in body-fixed coordinates, and $\mathbf{S}(\boldsymbol{\omega})$ is the skew-symmetric matrix such that $\mathbf{S}(\boldsymbol{\omega})\boldsymbol{x}$ is the cross product $\boldsymbol{\omega} \times \boldsymbol{x}$.

The DVL provides, without bottom-lock, relative velocity readings $\mathbf{v}_r(t) \in \mathbb{R}^3$, such that $\mathbf{v}(t) = \mathbf{v}_r(t) + \mathbf{v}_c(t)$, where $\mathbf{v}_c(t)$ corresponds to the ocean current velocity, expressed in body-fixed coordinates. It is assumed that the inertial ocean current is constant. The triad of orthogonally mounted rate gyros provides the angular velocity of the vehicle corrupted by rate gyro bias, all expressed in body-fixed coordinates, as given by $\boldsymbol{\omega}_m(t) = \boldsymbol{\omega}(t) + \mathbf{b}_{\boldsymbol{\omega}}(t)$, where $\mathbf{b}_{\boldsymbol{\omega}}(t) \in \mathbb{R}^3$ is the rate gyro bias. Finally, let $\mathbf{s}_i \in \mathbb{R}^3$, $i = 1, \ldots, N$, denote the inertial positions of the landmarks, and $\mathbf{a}_i \in \mathbb{R}^3$, $i = 1, \ldots, M$, the positions of the array of receivers of the USBL relative to the origin of $\{B\}$, expressed in body-fixed coordinates. Then, the range measurement between the i-th landmark and the j-th acoustic receiver of the USBL is given by

$$r_{i,j}(t) = \|\mathbf{s}_i - \mathbf{p}(t) - \mathbf{R}(t)\mathbf{a}_j\| \in \mathbb{R}. \tag{1}$$

B. Long Baseline / Ultra Short Baseline configuration

Long Baseline acoustic configurations are one of the earliest methods employed for underwater navigation. These are characterized by the property that the distance between the transponders is long or similar to the distance between the vehicle and the transponders. This is in contrast with Ultra Short Baseline systems, where the distance between the transponder and the vehicle is much larger than the distance between receivers of the USBL system. In common is the fact that, under standard assumptions, both the inertial position of the vehicle (for the LBL) and the position of the landmarks with respect to the vehicle, expressed in body-fixed coordinates, (for the USBL, in the so-called inverted configuration) are uniquely determined. This happens with the following standard assumption, which is considered in the remainder of the paper.

Assumption 1: The LBL/USBL acoustic positioning system includes at least 4 noncoplanar landmarks and 4 noncoplanar receivers.

III. Attitude and Heading Reference System

A. Attitude and rate gyro bias observer

The design of an Attitude and Heading Reference System is briefly detailed in this section. Essentially, after identifying the appropriate setting for attitude estimation, an algorithm previously developed by the authors is directly applied, yielding globally exponentially stable error dynamics.

Under Assumption 1, the USBL acoustic positioning system provides the position of each landmark relative to the vehicle and expressed in body-fixed coordinates, i.e.,

$$\mathbf{r}_i(t) := \mathbf{R}^T(t)\left[\mathbf{s}_i - \mathbf{p}(t)\right] \in \mathbb{R}^3, i = 1, \ldots, N.$$

Then, it is possible to define indirect measurements of the vector differences between landmarks as

$$\begin{cases} \mathbf{q}_1(t) := \mathbf{r}_1(t) - \mathbf{r}_2(t) \\ \mathbf{q}_2(t) := \mathbf{r}_1(t) - \mathbf{r}_3(t) \\ \vdots \\ \mathbf{q}_O(t) := \mathbf{r}_{N-1}(t) - \mathbf{r}_N(t) \end{cases},$$

where $O := n\left(n-1\right)/2$ is the number of 2-combinations of N elements, to which correspond the inertial vectors

$$\begin{cases} {}^I\mathbf{q}_1 := \mathbf{s}_1 - \mathbf{s}_2 \\ {}^I\mathbf{q}_2 := \mathbf{s}_1 - \mathbf{s}_3 \\ \vdots \\ {}^I\mathbf{q}_O := \mathbf{s}_{N-1} - \mathbf{s}_N \end{cases},$$

which are constant, such that ${}^I\mathbf{q}_i = \mathbf{R}(t)\mathbf{q}_i(t)$, $i = 1, \ldots, O$. Moreover, under Assumption 1, there exist at least two non-parallel vectors ${}^I\mathbf{q}_i$ and ${}^I\mathbf{q}_j$, $i, j \in \{1, \ldots, N\}$, $i \neq j$, and hence it is possible to estimate both the attitude and the rate gyro bias using one of the many solutions available in the literature.

In this paper, and in order to establish global properties for the overall navigation system, an attitude estimation solution previously proposed by the authors that has globally exponentially stable error dynamics is employed [23]. Let $\mathbf{x}_1(t)$ denote a column representation of the rotation matrix $\mathbf{R}(t)$, i.e.,

$$\mathbf{x}_1(t) = \begin{bmatrix} \mathbf{z}_1(t) \\ \mathbf{z}_2(t) \\ \mathbf{z}_3(t) \end{bmatrix} \in \mathbb{R}^9,$$

where

$$\mathbf{R}(t) = \begin{bmatrix} \mathbf{z}_1^T(t) \\ \mathbf{z}_2^T(t) \\ \mathbf{z}_3^T(t) \end{bmatrix},\ \mathbf{z}_i(t) \in \mathbb{R}^3,\ i = 1, \ldots, 3.$$

Define also the skew-symmetric matrix $\mathbf{S}_3\left(\mathbf{x}\right)$ as

$$\mathbf{S}_3\left(\mathbf{x}\right) := \textbf{blkdiag}\left(\mathbf{S}\left(\mathbf{x}\right), \mathbf{S}\left(\mathbf{x}\right), \mathbf{S}\left(\mathbf{x}\right)\right) \in \mathbb{R}^{9\times 9},\ \mathbf{x} \in \mathbb{R}^3,$$

and the constant matrix $\mathbf{C}_1$ as

$$\mathbf{C}_1 = \begin{bmatrix} {}^Iq_{11} & 0 & 0 & {}^Iq_{12} & 0 & 0 & {}^Iq_{13} & 0 & 0 \\ 0 & {}^Iq_{11} & 0 & 0 & {}^Iq_{12} & 0 & 0 & {}^Iq_{13} & 0 \\ 0 & 0 & {}^Iq_{11} & 0 & 0 & {}^Iq_{12} & 0 & 0 & {}^Iq_{13} \\ & & & & \vdots & & & & \\ {}^Iq_{O1} & 0 & 0 & {}^Iq_{O2} & 0 & 0 & {}^Iq_{O3} & 0 & 0 \\ 0 & {}^Iq_{O1} & 0 & 0 & {}^Iq_{O2} & 0 & 0 & {}^Iq_{O3} & 0 \\ 0 & 0 & {}^Iq_{O1} & 0 & 0 & {}^Iq_{O2} & 0 & 0 & {}^Iq_{O3} \end{bmatrix},$$

where ${}^I\mathbf{q}_i = \begin{bmatrix} {}^Iq_{i1} & {}^Iq_{i2} & {}^Iq_{i3} \end{bmatrix}^T \in \mathbb{R}^3$, $i = 1, \ldots, O$. Consider now the observer dynamics

$$\begin{cases} \dot{\hat{\mathbf{q}}}_1(t) = -\mathbf{S}\left(\boldsymbol{\omega}_m(t)\right)\hat{\mathbf{q}}_1(t) - \mathbf{S}\left(\mathbf{q}_1(t)\right)\hat{\mathbf{b}}_{\boldsymbol{\omega}}(t) \\ \qquad\qquad +\alpha_1\tilde{\mathbf{q}}_1(t) \\ \vdots \\ \dot{\hat{\mathbf{q}}}_O(t) = -\mathbf{S}\left(\boldsymbol{\omega}_m(t)\right)\hat{\mathbf{q}}_O(t) - \mathbf{S}\left(\mathbf{q}_O(t)\right)\hat{\mathbf{b}}_{\boldsymbol{\omega}}(t) \\ \qquad\qquad +\alpha_O\tilde{\mathbf{q}}_O(t) \\ \dot{\hat{\mathbf{b}}}_{\boldsymbol{\omega}}(t) = \sum_{i=1}^{O}\beta_i\mathbf{S}\left(\mathbf{q}_i(t)\right)\tilde{\mathbf{q}}_i(t) \\ \dot{\hat{\mathbf{x}}}_1(t) = -\mathbf{S}_3\left(\boldsymbol{\omega}_m(t) - \hat{\mathbf{b}}_{\boldsymbol{\omega}}(t)\right)\hat{\mathbf{x}}_1(t) \\ \qquad\qquad +\mathbf{C}_1^T\mathbf{Q}^{-1}\left[\mathbf{q}(t) - \mathbf{C}_1\hat{\mathbf{x}}_1(t)\right] \end{cases} \tag{2}$$

where $\alpha_i > 0, \beta_i > 0$, $i = 1, \ldots, O$, and $\mathbf{Q} \succ \mathbf{0}$ are observer parameters, and let $\tilde{\mathbf{q}}_i(t) := \mathbf{q}_i(t) - \hat{\mathbf{q}}_i(t)$, $i = 1, \ldots, O$, $\tilde{\mathbf{b}}_{\boldsymbol{\omega}}(t) := \mathbf{b}_{\boldsymbol{\omega}}(t) - \hat{\mathbf{b}}_{\boldsymbol{\omega}}(t)$, and $\tilde{\mathbf{x}}_1(t) := \mathbf{x}_1(t) - \hat{\mathbf{x}}_1(t)$ be the observer error. If $\operatorname{rank}\left(\mathbf{C}_1\right) = 9$, which is true under Assumption 1, then the origin of the observer error dynamics is a globally exponentially stable equilibrium point [23, Theorem 3]. An estimate of the rotation matrix is readily given by the 3×3 matrix representation of $\hat{\mathbf{x}}_1(t)$.

B. Refined attitude estimate

As previously mentioned, an estimate of the attitude is readily obtained from $\hat{\mathbf{x}}_1(t)$. However, as the topological restrictions of the Special Orthogonal Group are not explicitly enforced, the estimate thus obtained is not necessarily an element of $SO(3)$. This is not a problem when it comes to feed a filter for the linear motion quantities, as it will be seen in Section IV. However, in some applications, an explicit estimate on $SO(3)$ of the attitude of the vehicle might be required. This can be easily obtained from $\hat{\mathbf{x}}_1(t)$ resorting to the following result [24, Theorem 7].

Theorem 1: Consider the estimate $\hat{\mathbf{R}}(t)$ obtained from the attitude observer (2), with globally asymptotically exponentially error dynamics. Further suppose that the initial estimate satisfies $\hat{\mathbf{R}}\left(t_0\right) \in SO(3)$ and define a new attitude estimate $\hat{\mathbf{R}}_f(t)$ of the rotation matrix $\mathbf{R}(t)$ as

$$\begin{cases} \hat{\mathbf{R}}_f(t) = \arg\min\limits_{\mathbf{X}(t)\in SO(3)}\left\|\mathbf{X}(t) - \hat{\mathbf{R}}(t)\right\|, \left\|\hat{\mathbf{R}}^T(t)\hat{\mathbf{R}}(t) - \mathbf{I}\right\| \leq \epsilon \\ \dot{\hat{\mathbf{R}}}_f(t) = \hat{\mathbf{R}}_f(t)\mathbf{S}\left(\boldsymbol{\omega}(t)\right), \left\|\hat{\mathbf{R}}^T(t)\hat{\mathbf{R}}(t) - \mathbf{I}\right\| > \epsilon \end{cases},$$

where $\epsilon > 0$. Then,

1) $\hat{\mathbf{R}}_f(t) \in SO(3)$;
2) there exists t_s such that $\left\|\hat{\mathbf{R}}^T(t)\hat{\mathbf{R}}(t) - \mathbf{I}\right\| \leq \epsilon$ for all $t \geq t_s$ and therefore $\hat{\mathbf{R}}_f(t)$ corresponds to the projection on $SO(3)$ of $\hat{\mathbf{R}}(t)$ for all $t \geq t_s$; and
3) the error $\tilde{\mathbf{R}}_f(t) := \left\|\mathbf{R}(t) - \hat{\mathbf{R}}_f(t)\right\|$ is bounded and $\lim_{t\to\infty}\left\|\tilde{\mathbf{R}}_f(t)\right\| = 0$. Moreover, the convergence is exponentially fast.

IV. Cascade Navigation System

This section presents the overall navigation system. Firstly, a simple filter for the estimation of linear motion quantities (inertial position and ocean current) is introduced in Section IV-A. Afterwards, the complete cascade navigation system is described in Section IV-B and its stability is detailed.

A. Position and Velocity Filter

Assuming that the rotation matrix is known, it is straightforward to determine the inertial position of the vehicle from the LBL/USBL measurements. From (1) it is possible to write

$$2\frac{(\mathbf{s}_i-\mathbf{s}_j)^T}{r_{i,k}(t)+r_{j,k}(t)}\mathbf{p}(t) = -\left[r_{i,k}(t)-r_{j,k}(t)\right] + \frac{\|\mathbf{s}_i\|^2-\|\mathbf{s}_j\|^2-2(\mathbf{s}_i-\mathbf{s}_j)^T\mathbf{R}(t)\mathbf{a}_k}{r_{i,k}(t)+r_{j,k}(t)} \tag{3}$$

and

$$2\frac{(\mathbf{a}_m-\mathbf{a}_n)^T\mathbf{R}^T(t)}{r_{i,m}(t)+r_{i,n}(t)}\mathbf{p}(t) + r_{i,m}(t) - r_{i,n}(t) - \frac{\|\mathbf{a}_m\|^2-\|\mathbf{a}_n\|^2-2(\mathbf{a}_m-\mathbf{a}_n)^T\mathbf{R}^T(t)\mathbf{s}_i}{r_{i,m}(t)+r_{i,n}(t)} \tag{4}$$

for all $i,j=1,\ldots,N$, $i\neq j$, and $m,n=1,\ldots,M$, $m\neq n$. Grouping (3) and (4) gives $\mathbf{M}(t)\mathbf{p}(t)=\mathbf{m}(t)$, where $\mathbf{M}(t)$ is a full rank matrix under Assumption 1 for all t. Defining the cost function

$$J(t) = \left[\mathbf{M}(t)\mathbf{p}(t)-\mathbf{m}(t)\right]^T\mathbf{D}\left[\mathbf{M}(t)\mathbf{p}(t)-\mathbf{m}(t)\right],$$

where $\mathbf{D}$ is a positive definite matrix, the position that best explains the measurements is given by

$$\mathbf{p}(t) = \left[\mathbf{M}^T(t)\mathbf{D}\mathbf{M}\right]^{-1}\mathbf{M}^T(t)\mathbf{D}\mathbf{m}(t).$$

The system dynamics associated with the linear motion quantities is given by the linear time invariant system

$$\begin{cases}\dot{\mathbf{p}}(t) = {}^I\mathbf{v}_c(t)+\mathbf{u}(t)\\ {}^I\dot{\mathbf{v}}_c(t)=\mathbf{0}(t)\\ \mathbf{y}(t)=\mathbf{p}(t)\end{cases},$$

with $\mathbf{u}(t)=\mathbf{R}(t)\mathbf{v}_r(t)$. A simple solution is given by the steady-state Kalman filter, with GES error dynamics.

B. Stability Analysis

The structure of the complete navigation system, based on a combined LBL/USBL acoustic positioning device, a Doppler Velocity Log, and a triad of orthogonally mounted rate gyros is presented in Fig. 2. The LBL/USBL ranges and range differences of arrival are employed to compute the USBL fixes, which are the positions of the landmarks relative to the vehicle, expressed in body-fixed coordinates, $\mathbf{r}_i(t)$, $i=1,\ldots,N$. These, together with the angular velocity measurements, $\boldsymbol{\omega}_m(t)$, are the input of the AHRS, which in turn provides estimates of the attitude of the vehicle, encoded in $\hat{\mathbf{R}}(t)$, and the rate gyro bias, $\hat{\mathbf{b}}(t)$. An estimate of the angular velocity is then obtained as $\hat{\boldsymbol{\omega}}(t):=\boldsymbol{\omega}_m(t)-\hat{\mathbf{b}}_{\boldsymbol{\omega}}(t)$. The attitude estimate is employed, together with the LBL/USBL ranges and range differences of arrival, to obtain an algebraic inertial position. This estimate, together with the relative velocity $\mathbf{v}_r(t)$, provided by the DVL, and the attitude estimate $\hat{\mathbf{R}}(t)$ are the inputs of the position and velocity filter. This filter provides a filtered estimate of the inertial position of the vehicle, $\hat{\mathbf{p}}(t)$, and an estimate of the ocean current velocity, $\hat{\mathbf{v}}_c(t)$. An estimate of the linear velocity of the vehicle is then obtained as $\hat{\mathbf{v}}(t):=\mathbf{v}_r(t)+\hat{\mathbf{v}}_c(t)$.

The navigation system depicted in Fig. 2 is a cascade system. The stability of the error dynamics of the AHRS has already been detailed in Section III, and it is shown that the error dynamics are globally exponentially stable, i.e., $\tilde{\mathbf{R}}(t)$ and $\tilde{\mathbf{b}}_{\boldsymbol{\omega}}(t)$ converge globally exponentially fast to zero.

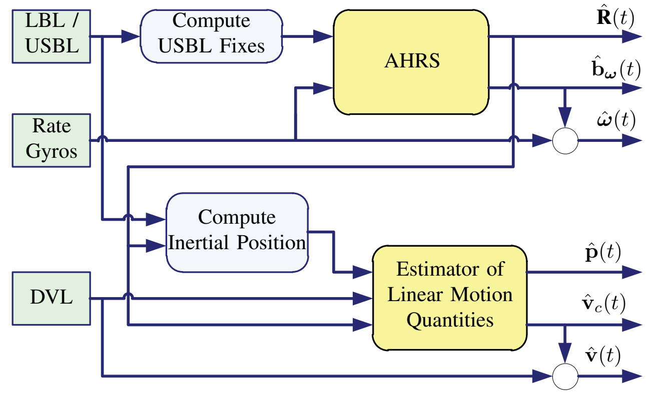

Fig. 2. Overall navigation system

Assuming exact attitude and position fixes, the linear motion estimator also has GES error dynamics. However, estimates of the attitude and the position are employed, whose error converges to zero exponentially fast. As a result, the error dynamics of the cascade position and velocity filter, which is linear time invariant, are also GES.

V. Simulation Results

This section presents extensive simulation results in order to evaluate the performance of the proposed navigation system. In the simulations a kinematic 3-D model of an underwater vehicle was employed for the sake of simplicity. The fact that the full nonlinear dynamics of the vehicle were not employed does not diminish, in any way, the validity of the results as all the filters are based on the kinematics of the vehicle only, which are exact.

The trajectory described by the vehicle is depicted in Fig. 3 and it consists of typical lawn mower maneuvers. The LBL configuration is composed of 4 acoustic transponders and their inertial positions are $\mathbf{s}_1 = \begin{bmatrix}1000 & 0 & 0\end{bmatrix}^T$ (m), $\mathbf{s}_2 = \begin{bmatrix}0 & 1000 & 0\end{bmatrix}^T$ (m), $\mathbf{s}_3 = \begin{bmatrix}1000 & 1000 & 0\end{bmatrix}^T$ (m), $\mathbf{s}_4 = \begin{bmatrix}0 & 0 & 100\end{bmatrix}^T$ (m), while the positions of the USBL array receivers, in body-fixed coordinates, are $\mathbf{a}_1 = \begin{bmatrix}0 & 0 & 0\end{bmatrix}$ (m), $\mathbf{a}_2 = \begin{bmatrix}0 & 0.3 & 0\end{bmatrix}$ (m), $\mathbf{a}_3 = \begin{bmatrix}0.20 & 0.15 & 0.15\end{bmatrix}$ (m), $\mathbf{a}_4 =$

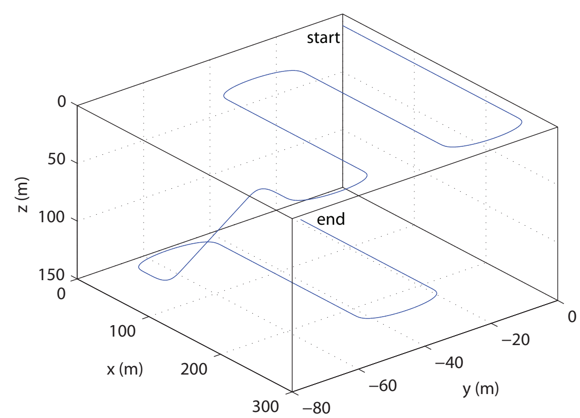

Fig. 3. Trajectory described by the vehicle

$\begin{bmatrix} 0.20 & 0.15 & -0.15 \end{bmatrix}$ (m), hence Assumption 1 is satisfied.

Sensor noise was considered for all sensors. In particular, the LBL range measurements, the USBL range differences of arrival, and the DVL relative velocity readings are assumed to be corrupted by additive uncorrelated zero-mean white Gaussian noise, with standard deviations of $1\,\mathrm{m}$, $6\times10^{-3}\,\mathrm{m}$, and $0.01\,\mathrm{m}$, respectively. The angular velocity measurements are also assumed to be perturbed by additive, zero mean, white Gaussian noise, with standard deviation of 0.05 °/s. The positions of the landmarks relative to the vehicle and expressed in body-fixed coordinates, $\mathbf{r}_i(t)$, are obtained from the LBL and USBL measurements considering the planar wave assumption, which yields excellent results as long as the distance between the landmarks and the vehicle is sufficiently large when compared with the distance between pairs of receivers of the USBL, see [26] for an example of a control application with the USBL that resorts to the same approximation. If anything, the employment of the exact solution for the position of the landmarks from the USBL and LBL readings would only improve on the present results.

To tune the Kalman filter for linear motion estimation, the state disturbance intensity matrix was chosen as $\mathbf{blkdiag}\left(10^{-2}\mathbf{I},\, 10^{-4}\mathbf{I}\right)$ and the output noise intensity matrix as $\mathbf{blkdiag}\,(10, 10, 100)$. The initial conditions were set to zero for all states. To tune the AHRS, the observer gains were chosen as $\alpha_i = 1$, $\beta_i = 10^{-8}$, $i = 1, \ldots, 6$, and $\mathbf{Q} = 10^5$. The initial rate gyro bias estimate was set to zero and the initial attitude estimate was set to $\mathbf{R}(0) = \mathbf{blkdiag}\,(-1, -1, 1)$.

In order to evaluate the performance of the attitude observer, and for the purpose of performance evaluation only, an additional error variable is defined as $\tilde{\mathbf{R}}_p(t) = \mathbf{R}^T(t)\hat{\mathbf{R}}(t)$, which corresponds to the rotation matrix error. Using the Euler angle-axis representation for this new error variable,

$$\begin{aligned}\tilde{\mathbf{R}}_p(t) &= \mathbf{I}\cos\left(\tilde{\theta}(t)\right) + \left[1-\cos\left(\tilde{\theta}(t)\right)\right]\tilde{\mathbf{d}}(t)\tilde{\mathbf{d}}^T(t)\\ &\quad -\mathbf{S}\left(\tilde{\mathbf{d}}(t)\right)\sin\left(\tilde{\theta}(t)\right),\end{aligned}$$

where $0 \leq \tilde{\theta}(t) \leq \pi$ and $\tilde{\mathbf{d}}(t) \in \mathbb{R}^3$, $\left\|\tilde{\mathbf{d}}(t)\right\| = 1$, are the angle and axis that represent the rotation error, the performance of the AHRS is identified with the evolution of $\tilde{\theta}$.

The convergence of the AHRS is very fast, as it is possible to observe from the evolution of the angle error $\tilde{\theta}(t)$ and the rate gyro bias error, which are depicted in Figs. 4 and 5, respectively. Although it is not shown due to the lack of space, the angle error remains below 1 degree for most of the time, which is a very good result, while the rate gyro bias error is confined to a very tight interval, below 0.02 °/s. The initial convergence of the position and velocity error is depicted in Fig. 6, which is also very fast. While all the errors are very small, the most interesting fact is that the errors along the z-axis are much larger when compared with those along the x and y axes. This is directly related to the

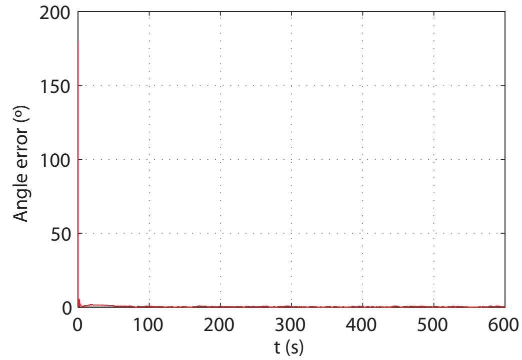

Fig. 4. Initial convergence of the attitude angle error

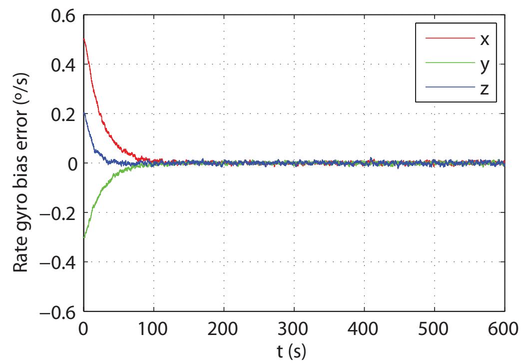

Fig. 5. Initial convergence of the rate gyro bias error

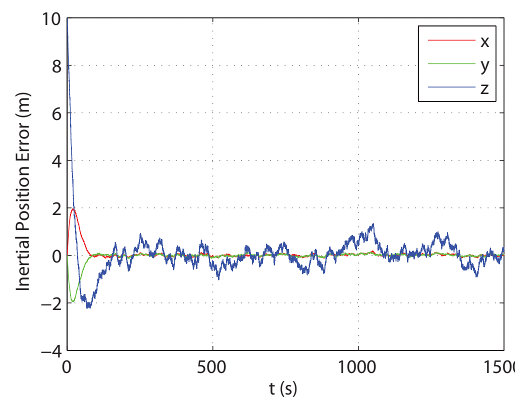

(a) Position error

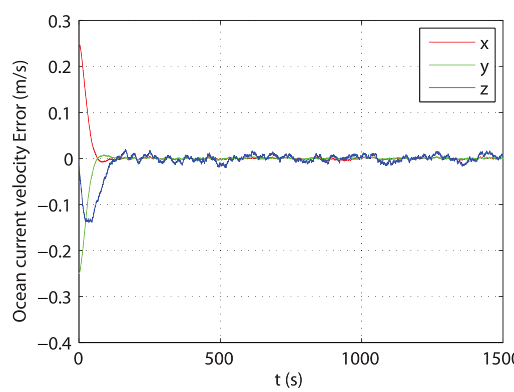

(b) Velocity error

Fig. 6. Initial convergence of error

TABLE I

STANDARD DEVIATION OF THE STEADY-STATE ESTIMATION ERROR, AVERAGED OVER 1000 RUNS OF THE SIMULATION

Variable	Standard deviation
$\tilde{\mathbf{p}}_x$ (m)	4.4×10^{-2}
$\tilde{\mathbf{p}}_y$ (m)	4.0×10^{-2}
$\tilde{\mathbf{p}}_z$ (m)	35×10^{-2}
$\tilde{\mathbf{v}}_x$ (m/s)	1.6×10^{-3}
$\tilde{\mathbf{v}}_y$ (m/s)	1.4×10^{-3}
$\tilde{\mathbf{v}}_z$ (m/s)	6.7×10^{-3}
$\tilde{\mathbf{b}}_{\boldsymbol{\omega}x}$ (°/s)	4.6×10^{-3}
$\tilde{\mathbf{b}}_{\boldsymbol{\omega}y}$ (°/s)	4.5×10^{-3}
$\tilde{\mathbf{b}}_{\boldsymbol{\omega}z}$ (°/s)	5.2×10^{-3}

structure and baseline of the LBL array: the baseline along x and y is roughly 10 times the baseline along z.

Finally, in order to better evaluate the performance of the proposed solution, the Monte Carlo method was applied, and 1000 simulations were carried out with different, randomly generated noise signals. The standard deviation of the errors were computed for each simulation and averaged over the set of simulations. The results are depicted in Table I. The mean attitude angle error is 0.35 °. As it is possible to observe, the standard deviation of the errors is very low, adequate for the sensor suite that was considered.

VI. CONCLUSIONS

This paper presented a novel integrated navigation system based on a combined Long Baseline / Ultra-Short Baseline acoustic positioning system. First, a novel Attitude and Heading Reference System for underwater vehicles, based on the LBL/USBL, in addition to rate gyro measurements, was proposed, hence avoiding the use of magnetometers that can yield bad results when operating near structures with a strong magnetic signature. Afterwards, a simple filter for the estimation of linear motion quantities (inertial position and ocean current velocity) was proposed, which resorts also to a DVL. The stability of the resulting cascade system error dynamics was analyzed and it was shown that the origin is a globally exponentially stable equilibrium point. Finally, simulation results were presented that illustrate the achievable performance of the overall navigation system.

REFERENCES

[1] L. Whitcomb, D. Yoerger, and H. Singh, "Combined Doppler/LBL Based Navigation of Underwater Vehicles," in *Proceedings of the the 11th International Symposium on Unmanned Untethered Submersible Technology*, Durham, USA, Aug. 1999.

[2] J. Jouffroy and J. Opderbecke, "Underwater vehicle trajectory estimation using contracting PDE-based observers," in *Proceedings of the 2004 American Control Conference*, vol. 5, Boston, MA, USA, Jun-July 2004, pp. 4108–4113.

[3] J. Kinsey and L. Whitcomb, "Preliminary field experience with the DVLNAV integrated navigation system for manned and unmanned submersibles," in *Proceedings of the 1st IFAC workshop on guidance and control of underwater vehicles*, Newport, South Wales, UK, Apr. 2003, pp. 83–88.

[4] M. Larsen, "Synthetic long baseline navigation of underwater vehicles," in *Proceedings of the 2000 MTS/IEEE Oceans*, vol. 3, Providence, RI, USA, Sep. 2000, pp. 2043–2050.

[5] J. Vaganay, J. Bellingham, and J. Leonard, "Comparison of fix computation and filtering for autonomous acoustic navigation," *International Journal of Systems Science*, vol. 29, no. 10, pp. 1111–1122, Oct. 1998.

[6] P. Batista, C. Silvestre, and P. Oliveira, "Optimal position and velocity navigation filters for autonomous vehicles," *Automatica*, vol. 46, no. 4, pp. 767–774, Apr. 2010.

[7] M. Morgado, P. Oliveira, C. Silvestre, and J. Vasconcelos, "USBL/INS Tightly-Coupled Integration Technique for Underwater Vehicles," in *Proceedings of the 9th International Conference on Information Fusion*, Florence, Italy, Jul. 2006.

[8] M. Morgado, P. Batista, P. Oliveira, and C. Silvestre, "Position USBL/DVLSensor-based Navigation Filter in the presence of Unknown Ocean Currents," *Automatica*, vol. 47, no. 12, pp. 2604–2614, Dec. 2011.

[9] M. Morgado, P. Oliveira, and C. Silvestre, "Design and experimental evaluation of an integrated USBL/INS system for AUVs," in *Proceedings of the 2010 IEEE International Conference on Robotics and Automation*, Anchorage, USA, May 2010, pp. 4264–4269.

[10] N. Metni, J.-M. Pflimlin, T. Hamel, and P. Soueres, "Attitude and gyro bias estimation for a VTOL UAV," *Control Engineering Practice*, vol. 14, no. 12, pp. 1511–1520, Dec. 2006.

[11] A. Tayebi, S. McGilvray, A. Roberts, and M. Moallem, "Attitude estimation and stabilization of a rigid body using low-cost sensors," in *Proceedings of the 46th IEEE Conference on Decision and Control*, New Orleans, USA, Dec. 2007, pp. 6424 –6429.

[12] D. Campolo, F. Keller, and E. Guglielmelli, "Inertial/Magnetic Sensors Based Orientation Tracking on the Group of Rigid Body Rotations with Application to Wearable Devices," in *Proceedings of the 2006 IEEE/RSJ International Conference on Intelligent Robots and Systems - IROS 2006*, Beijing, China, Oct. 2006, pp. 4762–4767.

[13] D. Choukroun, "Novel Results on Quaternion Modeling and Estimation from Vector Observations," in *Proceedings of the AIAA Guidance Navigation and Control Conference*, Chicago, IL, USA, Aug. 2009.

[14] A. Sabatini, "Quaternion-based extended Kalman filter for determining orientation by inertial and magnetic sensing," *IEEE Transactions on Biomedical Engineering*, vol. 53, no. 7, pp. 1346–1356, Jul. 2006.

[15] A. Sanyal, T. Lee, M. Leok, and N. McClamroch, "Global optimal attitude estimation using uncertainty ellipsoids," *Systems & Control Letters*, vol. 57, no. 3, pp. 236–245, Mar. 2008.

[16] J. Vasconcelos, R. Cunha, C. Silvestre, and P. Oliveira, "Landmark Based Nonlinear Observer for Rigid Body Attitude and Position Estimation," in *Proceedings of the 46th IEEE Conference on Decision and Control*, New Orleans, LA, USA, Dec. 2007, pp. 1033–1038.

[17] H. Rehbinder and B. Ghosh, "Pose Estimation Using Line-Based Dynamic Vision and Inertial Sensors," *IEEE Transactions on Automatic Control*, vol. 48, no. 2, pp. 186–199, Feb. 2003.

[18] R. Mahony, T. Hamel, and J.-M. Pflimlin, "Nonlinear Complementary Filters on the Special Orthogonal Group," *IEEE Transactions on Automatic Control*, vol. 53, no. 5, pp. 1203–1218, Jun. 2008.

[19] J. Thienel and R. Sanner, "A Coupled Nonlinear Spacecraft Attitude Controller and Observer With an Unknown Constant Gyro Bias and Gyro Noise," *IEEE Transactions on Automatic Control*, vol. 48, no. 11, pp. 2011–2015, Nov. 2003.

[20] P. Martin and E. Salaun, "Design and implementation of a low-cost observer-based attitude and heading reference system," *Control Engineering Practice*, vol. 17, no. 7, pp. 712–722, Jul. 2010.

[21] J. Crassidis, F. Markley, and Y. Cheng, "Survey of Nonlinear Attitude Estimation Methods," *Journal of Guidance, Control and Dynamics*, vol. 30, no. 1, pp. 12–28, Jan.-Feb. 2007.

[22] P. Batista, C. Silvestre, and P. Oliveira, "Sensor-based Globally Asymptotically Stable Filters for Attitude Estimation: Analysis, Design, and Performance Evaluation," *IEEE Transactions on Automatic Control*, vol. 57, no. 8, pp. 2095–2100, Aug. 2012.

[23] ——, "Globally Exponentially Stable Cascade Observers for Attitude Estimation," *Control Engineering Practice*, vol. 20, no. 2, pp. 148–155, Feb. 2012.

[24] ——, "A GES Attitude Observer with Single Vector Observations," *Automatica*, vol. 48, no. 2, pp. 388–395, Feb. 2012.

[25] S. Bhat and D. Bernstein, "A topological obstruction to continuous global stabilization of rotational motion and the unwinding phenomenon," *Systems & Control Letters*, vol. 39, no. 1, pp. 63–70, 2000.

[26] P. Batista, C. Silvestre, and P. Oliveira, "A time differences of arrival based homing strategy for autonomous underwater vehicles," *International Journal of Robust and Nonlinear Control*, vol. 20, no. 15, pp. 1758–1773, Oct. 2010.